Joint Pathology Center
Veterinary Pathology Services

WEDNESDAY SLIDE CONFERENCE
2020-2021

Conference 4

16 September, 2020

Joint Pathology Center
Silver Spring, Maryland

CASE 1: 18/530 (4137582-00)

Signalment: 2 years, female, Norwegian kystgeit, *Capra hircus*, goat.

History:
The goat was from a small flock of 15 Norwegian kystgeit, which is an old goat breed kept historically for meat production. The flock was kept on a barren pasture due to an unusually dry and warm summer. The goat was examined several times during a period of two weeks. The goat was lethargic and very thin, had poor appetite and was lying down. There were no respiratory or gastrointestinal signs, and the feces had normal consistency. Blood samples showed hypocalcemia, hypomagnesemia, and anemia. The goat was treated with calcium, magnesium, NSAIDs and penicillin.

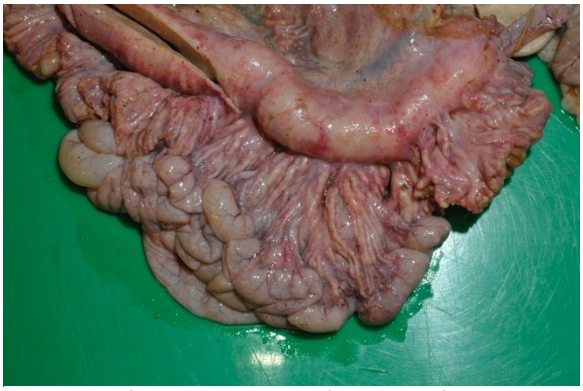

Intestine and mesentery, goat: The most striking gross lesion is severe granulomatous and caseating mesenteric lymphadenitis and thick rope-like lymphatics. (Photo courtesy of: Norwegian University of Life Sciences, Faculty of Veterinary Medicine, PO Box 369 Sentrum, 0102 Oslo, Norway)

Gross Pathology:
Subcutaneous tissues on extremities, the body and ventrally on the head were moist due to edema. Mucosal membranes were pale. The chest cavity contained 100 mL transudate, and lungs were congested and edematous with abundant frothy fluid in trachea and bronchi. Epicardial fat had partially gelatinous and moist appearance. The rumen was moderately filled with normal content. The abomasal wall was thickened due to severe submucosal edema.

The mesenteric lymph nodes were severely enlarged with caseous necrosis which usually affected the entire cut surface of the nodes. Some nodes had a dark red cut surface with multiple grey to white, up to 0.5 cm large nodules. Mesenterial lymphatics were severely thickened, grey to white in color, and firm.

Severe lesions were present in the small intestine, starting 4 meters aborally to the pylorus, and continuing to and including the ileocecal opening. In the jejunum there were multifocal, up to 0.5 cm large, grey to white nodules in the mucosa. Ileum had a diffusely thickened wall,

Intestine and mesentery, goat: A severe granulomatous lymphangitis. (Photo courtesy of: Norwegian University of Life Sciences, Faculty of Veterinary Medicine, PO Box 369 Sentrum, 0102 Oslo, Norway)

with a grey to white necrotic mucosa. The aboral small intestine had small amounts of watery and blood tinged content. Nodules in the intestinal wall had a caseous center. The serosa of affected small intestine had multiple small white nodules. In the colon there were sparse amounts of normal intestinal content.

Laboratory results:
On initial bacteriological culture from ileum and mesenterial lymph node, a mixed bacterial flora of *Escherichia coli*, hemolytic *Escherichia coli* and *Enterococcus* sp. were detected. Mycobacteriological culture from small intestinal content and mesenterial lymph node showed growth of *Mycobacterium avium* subsp. *hominissuis*. Small intestinal content investigated by real time PCR was positive for the same bacterium. Bacteriological culture and PCR was negative for *Mycobacterium avium* subsp. *paratuberculosis*.

Microscopic description:
The mucosa of the small intestine is mostly missing, due to a combination of autolytic changes and necrosis. In remnants of mucosa there is a diffuse infiltration of neutrophils and macrophages and some lymphocytes and plasma cells. In the submucosa there are distinct multifocal to confluent areas dominated by macrophages and neutrophils in areas interpreted to be remnants of gut-associated lymphoid tissue, some of which have necrotic centers. Between these, there is a diffuse infiltration of macrophages, neutrophils, lymphocytes and plasma cells.

In the serosa and in the mesentery, there are multiple granulomas with necrotic centers surrounded by a rim of macrophages and some neutrophils, surrounded by infiltration of lymphocytes and plasma cells. With increasing size of the granulomas there are increasing fibroblast proliferation in the periphery. Several granulomas have large vacuoles on the border between the necrotic center and the zone with macrophages and fibrosis. Some granulomas are associated with vascular structures, and areas of inflammation affected lymphatic vessels. Some granulomas have dystrophic mineralization in the center.

Ziehl-Neelsen stain revealed numerous intracellular acid-fast bacilli in macrophages.

Contributor's morphologic diagnosis:
Small intestine and mesentery: Multifocal to confluent granulomatous enteritis with serosal and mesenterial granulomatous lymphangitis with severe caseous necrosis.

Contributor's comment:
In the *Mycobacterium avium* complex (MAC), there are 9 species of slow-growing mycobacteria and a further subset of isolates of undetermined classification (the so-called "MAC-others").[6] The

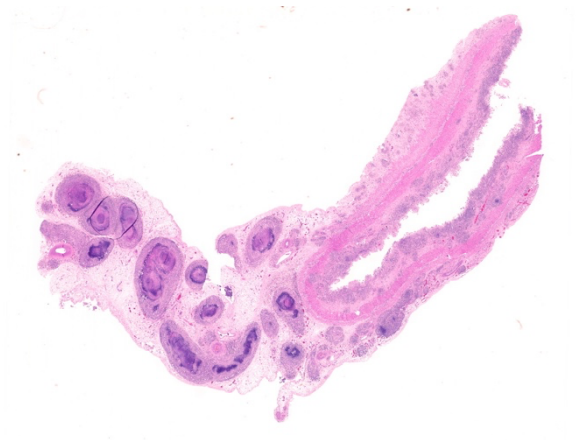

Intestine and mesentery, goat: The most striking subgross lesion of this case is the mesenteric granulomatous lymphangitis. Each granuloma represents a severely inflamed lymph vessel. (HE, 5X)

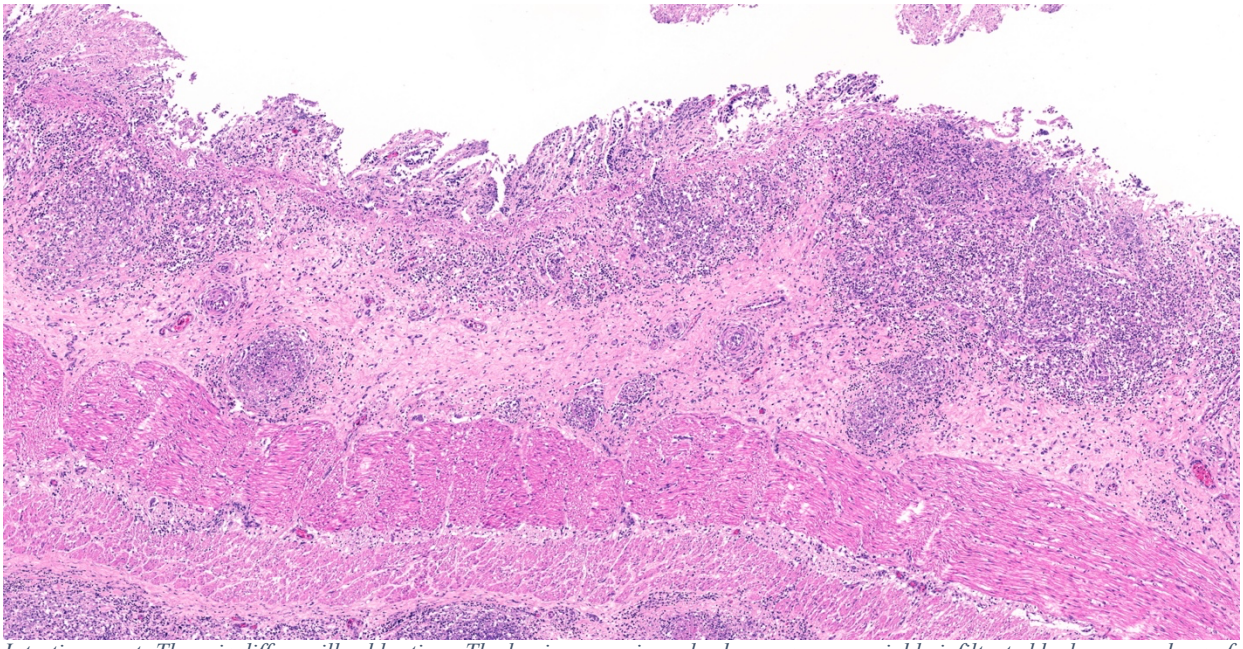

Intestine, goat: There is diffuse villar blunting. The lamina propria and submucosa are variably infiltrated by large numbers of macrophages and lymphocytes and a submucosal lymphatic is effaced by a dense lymphohistiocytic infiltrate. (HE, 160X)

species *Mycobacterium (M.) avium* contain four distinct subspecies; *M. avium* subsp. *hominissuis* (MAH), *M. avium* subsp. *paratuberculosis* (MAP), *M. avium* subsp. *avium* (MAA), and *M. avium* subsp. *silvaticum* (MAS). Although closely related, theses subspecies represent distinct organisms, each with specific pathogenic and host range characteristics. They range from environmental opportunistic bacteria that cause infections in swine and immunocompromised human patients, to pathogens of birds and ruminants.[6] The MAH was quite recently suggested as a separate subspecies, to reflect the distinction of human and porcine isolates from bird-type strains.[5]

Paratuberculosis, caused by MAP and characterized by chronic wasting in goats, was suspected due to the clinical signs and the gross pathology observed at necropsy. However, culture and PCR were negative for this bacterium and MAH was cultured and detected by PCR.

MAH is an environmental opportunistic pathogen for humans and swine worldwide, but the organism has also been isolated from numerous other animals, such as cattle, dogs, birds, deer and horses.[6] MAH has also been shown to be able to cause disease in goats after experimental oral infection, characterized by a large variety of granulomas in organized gut-associated tissues and intestinal lymph nodes. In severely sick goats, 2-3 months post infection, there were granulomas with extensive necrosis, little mineralization and variable numbers of acid-fast bacteria, surrounded by many CD4+ T cells, but only few epithelioid macrophages.[7] As the granulomas develop with time, they were characterized with a granuloma stage 1-6, and in

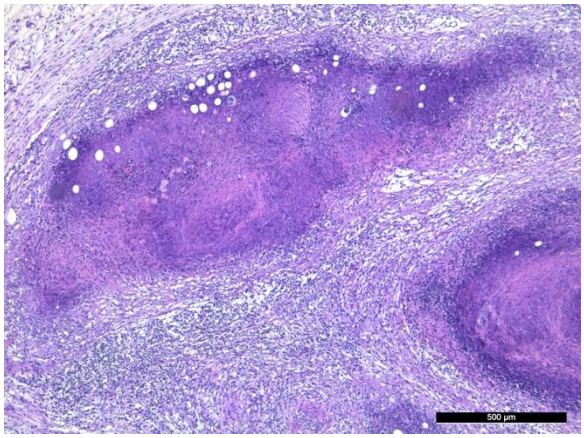

Mesentery, goat: Low magnification of severely inflamed mesenteric lymphatics. Well-formed granulomas efface mesenteric lymphatics. (HE, 40X) (Photo courtesy of: Norwegian University of Life Sciences, Faculty of Veterinary Medicine, PO Box 369 Sentrum, 0102 Oslo, Norway)

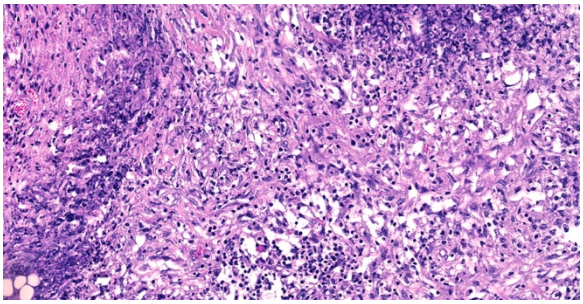

Mesentery, goat: Higher magnification of a granuloma effacing a lymphatic. The center of granuloma (at left) is composed of eosinophilic granular debris surrounded by a basophilic band of nuclear debris. Surrounding this are layers of epithelioid macrophages admixed with fewer lymphocytes, neutrophils and cellular debris, enmeshed in lamellated bands of mature collagen (HE 350X).

the older granulomas there is more extensive caseous necrosis, fewer epithelioid macrophages and multinucleated giant cells, more distinct fibrosis and more lymphocytes,[7] characteristics consistent with lesions in the present case. Many of the granulomas in the present case, both in the serosa and the mesentery, had extensive necrosis, but mineralization was only seen in a few granulomas. Two out of three sections from the mesenterial lymph node from the present case had total necrosis of the lymph node, surrounded by a thick zone of connective tissue. The third section of the mesenterial lymph node had severe multifocal to confluent necrosis.

Soil and water are considered to be the natural reservoirs for MAH. Drinking water and tap aerosols are thought to be the main source for human infections, and for swine the source may be drinking water, feed, bedding materials, soil, wastewater, invertebrates and possibly other materials.[6]

A study of genotypes and strain distribution of MAH isolated from humans and pigs in Belgium revealed a large genetic diversity of strains and an absence of a link between genotypes and the place of residence (human) or the farm or origin (pigs), suggesting an environmental source of infection.[8]

The flock with the submitted case was held on a barren pasture, due to unusual and severe drought and warm weather in Norway in the summer of 2018. It is possible that the weather and pasture conditions may have contributed to an increased likelihood of an oral infection with MAH, however to the contributor's knowledge, this was the only documented case of MAH induced disease in animals in the country that summer.

Contributing Institution:
Norwegian University of Life Sciences
Faculty of Veterinary Medicine
PO Box 369 Sentrum
0102 Oslo
Norway

JPC diagnosis:
Small intestine, mesentery: Lymphangitis, granulomatous, multifocal to coalescing, chronic, severe, with neutrophilic and histiocytic enteritis, Norwegian kystgeit, caprine.

JPC comment:
There was spirited debate during the conference about the neutrophil content in some of these lesions. While acid fast stains revealed numerous acid-fast bacilli in macrophages as expected, the autolysis of the tissue section may have obscured an additional neutrophilic process.

The contributor summarizes the current classification of *Mycobacterium avian* spp succinctly. While the discussed four subspecies affect veterinary species, the remaining identified species in "MAC" primarily affect humans (*M. intracellulare*, *M. colombiense*, *M. chimaera*, *M. marseillense*, *M. timonense*, *M.*

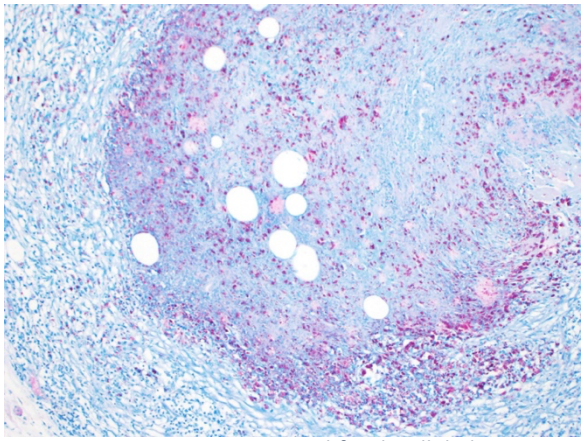

Mesentery, goat: Numerous acid-fast bacilli-laden macrophages are present within the lumen of a lymphatic. (Fite-Faraco, 100X).

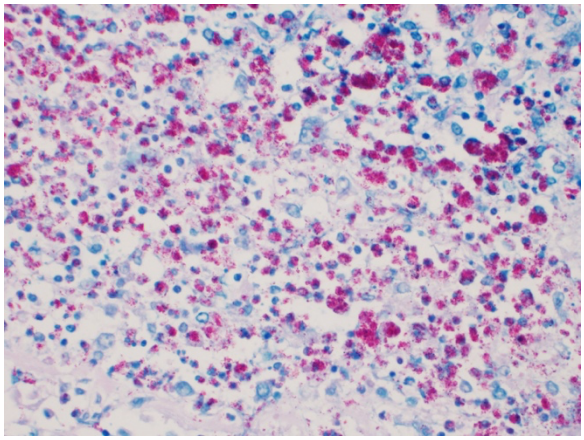

Intestine, goat: Higher magnification of bacilli-laden macrophages demonstrating the density of bacilli within each macrophage. (Fite-Faraco, 400X)

boucherdurhonense, *M. vulneris*, *M. arosiense*, and "MAC-others").[1]

In contrast to *Mycobacterium tuberculosis*, Mycobacterium avian sp. express serovar specific glycopeptidolipids (ssGPL), which play a role in inhibiting macrophages activation, and in immunomodulatory activity by downregulating Th_1 response. Gene *lysX* (lysyl-transferase-lysyl-tRNA synthetase) is involved in the lysinylation of surface phospholipids, which makes the bacterium susceptible to antimicrobial peptides. Wild type, mutated, or absent *lysX* genes affect many aspects of virulence, including rate of macrophage fusion, GPL expression and antigenic reactivity, susceptibility to defensins, and tolerance toward oxidative and nitrosative stress. The patterns of change in these factors is different between MAH and *Mycobacterium tuberculosis* but provides an interesting area of future research.[4]

Mycobacterium avium subspecies *hominissuis* was recently confirmed as the causative agent of disseminated disease in a cat in 2019. The species was confirmed by culture and single nucleotide polymorphism analysis, the first diagnosis of MAH confirmed by gene analysis.[2]
While MAH rarely causes disease in horses, a complete genome sequence of MAH was completed from the stomach contents of an equine abortion case in Japan in 2019.[3]

Two typical acid-fast stains are Ziehl-Neelsen and Fite-Faraco, and *Mycobacteria* spp. exhibit "acid-fastness" due to the high mycolic acid content in their cell walls. All *Mycobacterium* spp. have this property, but a number of *Actinomycetes* also have mycolic acid in their cell walls and have some degree of acid-fastness. Notable bacteria include *Nocardia* spp, and *Rhodococcus* spp, which are also pathogens of veterinary concern.

While not classified in MAC, *Mycobacterium tuberculosis* continues to be a problematic pathogen around the world. Noted historical figures Jane Austen, George Orwell, John Keats, Walt Whitman, Paul Gaugin, Frederic Chopin, several kings of France, and Florence Nightingale all suffered and died from tuberculosis. Even more recent figures, such as Ringo Starr experienced infection as a child and subsequently recovered.

In 1882, Robert Koch, a Prussian physician, used a new staining method and used it on sputum of afflicted people. He was the first person to visualize the pathogen *Mycobacterium tuberculosis*. His research on human tuberculosis was the foundation of his development of the framework known as "Koch's Postulates", which criteria to establish a causal relationship between a microbe and a disease. Sir Bradford Hill built upon Koch's Postulates and established 9 criteria for causation (Bradford Hill criteria) in 1965, which are debated, but often still applicable today.

References:

1. Eslami M, Shafiei M, Ghasemian A, et al. *Mycobacterium avium paratuberculosis* and *Mycobacterium avium* complex and related subspecies as causative agents of zoonotic and occupational diseases. *Journal of Cellular Physiology*. 2019;234(8):12415-12421.
2. Kanegi R, Yasugi M, Nabetani T, et al. Clinical findings and treatment of disseminated *Mycobacterium avium* subspecies *hominissuis* infection in a domestic cat. *Journal of Veterinary Medical Science*. 2019;81(12):1842-1849.
3. Kinoshita Y, Niwa H, Uchida-Fujii E, Nukada T. Complete genome sequence of *Mycobacterium avium* subsp. *hominissuis* strain JP-H-1, isolated

from an equine abortion case in Japan. *Microbiol Resour Announc*. 2019;8:e01228-19.
4. Kirubakar G, Schafer H, Rickerts V, Schwarz C, Lwein A. Mutation on *lysX* from *Mycobacteriumavium hominissuis* impacts the host-pathogen interaction and virulence phenotype. *Virulence*. 2020;11(1):132-144.
5. Mijs W, de Haas P, Rossau R, et al. Molecular evidence to support a proposal to reserve the designation *Mycobacterium avium* subsp. *avium* for bird-type isolates and '*M. avium* subsp. *hominissuis*' for the human/porcine type of *M. avium*. *Int J Syst Evol Microbiol.* 2002;52:1505-1518.
6. Rindi L, Garzelli C. Genetic diversity and phylogeny of *Mycobacterium avium*. *Infect Genet Evol.* 2014;21:375-383.
7. Schinköthe J, Köhler H, Liebler-Tenorio EM. Characterization of tuberculous granulomas in different stages of progression and associated tertiary lymphoid tissue in goats experimentally infected with *Mycobacterium avium* subsp. *hominissuis*. *Comp Immunol Microbiol Infect Dis.* 2016;47:41-51.
8. Vluggen C, Soetaert K, Duytschaever L, et al. Genotyping and strain distribution of *Mycobacterium avium* subspecies *hominissuis* isolated from humans and pigs in Belgium, 2011-2013. *Euro Surveill.* 2016;21:30111

CASE 2: 17-H43332 (4100929-00)

Signalment: 4-year-old, male, castrated, Yorkshire terrier dog (*Canis familiaris*)

History:
This dog presented for evaluation of chronic (1 year) right hind limb lameness that had recently become significantly worse – the dog was non-weight bearing on the right hindlimb. Additionally, the dog became lame on the left hind limb and was having significant trouble walking. Radiographs revealed moth-eaten lucencies of the left ischium, left acetabulum, left and right distal femurs, fabellae, right proximal tibia, right patella, caudal aspect of both scapulae, and a suspected pathologic fracture of the right tibial tuberosity. A *Blastomyces* urine antigen test was negative. Bloodwork revealed a hyperglobulinemia (total protein: 9.8 g/dL) and a fine needle aspirate of bone was inconclusive. The dog was originally from Arizona and had since moved to Illinois approximately four years ago.

Gross Pathology:
Musculature of the right hind limb was generally and moderately reduced compared to the left hind limb (atrophy). The right stifle joint was swollen with crepitus palpated upon extension, contains a moderate amount of thick, tan, opaque material, and the joint capsule is mildly thickened, tan, and granular. The distal portion of the right lateral femoral condyle was freely moveable and jagged (pathologic fracture). The trochlear ridges and condyles of the right and left femur were irregularly raised, roughened, translucent (thinned), and easily cut by a scalpel blade. The left and right ischiatic tuberosities were asymmetrical with the surface being slightly expanded, roughened, irregular, thinned, and easily cut by a scalpel blade. The dorsal half of the right scapula was also mildly expanded, roughened, thinned, and easily cut by a scalpel blade.

Radiography, dog: Radiographs revealed moth-eaten lucencies of the left ischium, left acetabulum, left and right distal femurs, fabellae, right proximal tibia, right patella, caudal aspect of both scapulae, and a suspected pathologic fracture of the right tibial tuberosity. (Photo courtesy of: University of Illinois College of Veterinary Medicine, Veterinary Diagnostic Laboratory, http://vetmed.illinois.edu/vet-resources/veterinary-diagnostic-laboratory/)

Stifle, dog: The right stifle joint was swollen with crepitus palpated upon extension, contains a moderate amount of thick, tan, opaque material, and the joint capsule is mildly thickened, tan, and granular. (Photo courtesy of: University of Illinois College of Veterinary Medicine, Veterinary Diagnostic Laboratory, http://vetmed.illinois.edu/vet-resources/veterinary-diagnostic-laboratory/)

The right popliteal and bilateral inguinal lymph nodes were markedly enlarged, firm, white, and granular on cut surface.

The lungs were diffusely mottled red to pink, soft, and contained multiple, randomly scattered, 1-3 mm diameter, white, semi-firm, nodules within all lung lobes. The pleural surface of the diaphragm, at the junction of the central tendon and muscle, contained several similar nodules.

The nasal cavity and brain were unremarkable.

Laboratory results:
A portion of joint capsule was submitted for aerobic and myocology culture which returned a light growth of *Coccidioides* sp. and very rare growth of *Pasteurella stomatis*.

The *Coccidioides* sp. isolate from mycology culture was identified by 18S rRNA gene sequencing with the top match being similar to *C. posadasii* (100%) but also with a very close homology to *C. immitis* (99%).

Microscopic description:
Bone (right femur and scapula): The medullary space is effaced and expanded by numerous coalescing nodules of mixed inflammation suspended in thin anastomosing bands of dense fibrous connective tissue. The inflammatory nodules comprise mostly epithelioid macrophages and rare neutrophils surrounded by a layer of lymphocytes and plasma cells and occasionally encapsulated by a thin band of fibrous connective tissue (granulomas). The center of granulomas is occasionally replaced by granular to amorphous (necrotic) debris and often contain at least one discrete fungal spherule. The spherules are 20-60 um in diameter characterized by a smooth, 5 um thick, refractile and hyaline, double-contoured wall and contain granular basophilic material or rarely a few 5-7 um diameter endospores. The trabecular and cortical bone are markedly thinned and often obliterated by the inflammation. The thin trabeculae of remaining bone are usually smooth, occasionally scalloped, and rarely lined by small numbers of osteoclasts located within Howship's lacunae. Within sections of the distal femur, the same inflammatory response obliterates the articular cartilage, extends into the joint space, and expands and effaces the synovium of the stifle joint. In the section of scapula, the inflammation

Scapula, dog: The dorsal half of the right scapula was also mildly expanded, roughened, thinned, and easily cut by a scalpel blade. (Photo courtesy of: University of Illinois College of Veterinary Medicine, Veterinary Diagnostic Laboratory, http://vetmed.illinois.edu/vet-resources/veterinary-diagnostic-laboratory/)

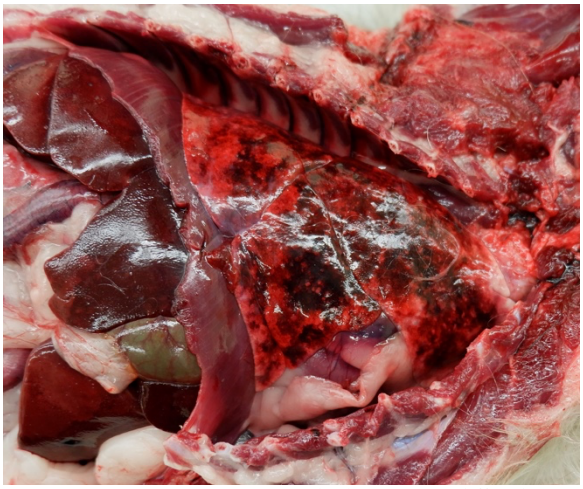

Thoracic viscera in situe, dog: The lungs were diffusely mottled red to pink, soft, and contained multiple, randomly scattered, 1-3 mm diameter, white, semi-firm, nodules within all lung lobes (Photo courtesy of: University of Illinois College of Veterinary Medicine, Veterinary Diagnostic Laboratory, http://vetmed.illinois.edu/vet-resources/veterinary-diagnostic-laboratory/)

multifocally obliterates the cortical bone and extends into the adjacent skeletal muscle.

Contributor's morphologic diagnosis:
Bone (right femur and scapula): Severe, chronic, multifocal, granulomatous osteomyelitis, arthritis, and synovitis, with extensive boney lysis and intralesional fungal spherules (consistent with *Coccidioides* sp).

Contributor's comment:
Coccidioides is a soil dwelling, dimorphic fungus that can cause systemic disease in a wide range of mammals, humans, and some reptiles.[13] Coccidioidomycosis is also known as San Joaquin Valley fever, valley fever, or desert fever and is endemic to semiarid regions of southern Arizona, California, New Mexico, Nevada, Utah, western Texas, northern Mexico, and Central and South America.[6,11,12] Distinction between two different phylogenetic clades based on genetic analysis suggests that there are two different species that cause disease including *Coccidioides immitis* and *Coccidioides posadasii*, however the biological relevance of this genetic variability is unclear.[3,5]

During periods of heavy rainfall, the dormant mycelium below the soil surface proliferates and extends to the surface where it produces infective spores (arthroconidia). When disturbed by animal activity, these infective arthroconidia are inhaled or, less commonly, come into contact with damaged skin, where only a few spores are required to initiate infection. After being inhaled, the arthrospores are phagocytosed in alveoli, which stimulates structural changes in the arthrospores to form into spherules. These spherules swell, undergo endosporulation, rupture, and release hundreds of endospores into the surrounding tissue. The newly released endospores mature into new spherules and the cycle is repeated within affected tissues.[3,6,12]

Because of the fungal life cycle, dogs in endemic areas that spend more time outdoors, have more land to roam, and exposed to dusty environments are at increased risk of infection. Other risk factors in dogs include a younger age, being a large breed, and working or sporting activity.[1,15] Clinical infection is commonly localized to the pulmonary system and associated lymph nodes resulting in chronic respiratory disease. However, when endospores enter the lymphatics or blood, tropism for bones, joints, and less frequently heart, brain, eyes, testes, skin, spleen, liver, and kidney create a wide range of clinical signs that can complicate antemortem diagnosis.[6] Dissemination can occur early in the disease process or months after initial infection, with the most common clinical presentations being neurological signs or lameness due to osteomyelitis. Diagnosis often relies on multiple

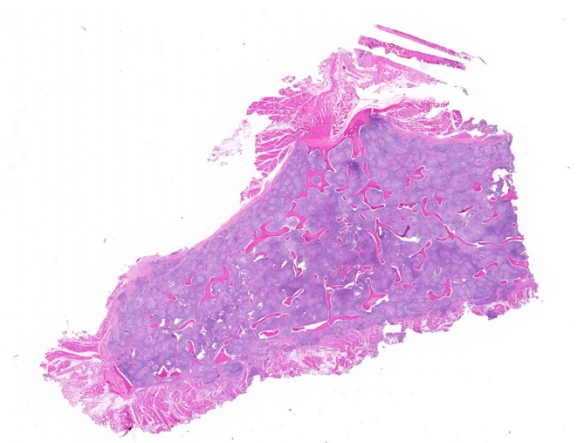

Bone, dog: At subgross magnification, the medulla of this section of bone is markedly hypercellular and there is a definite loss of medullary bone. (HE, 4X).

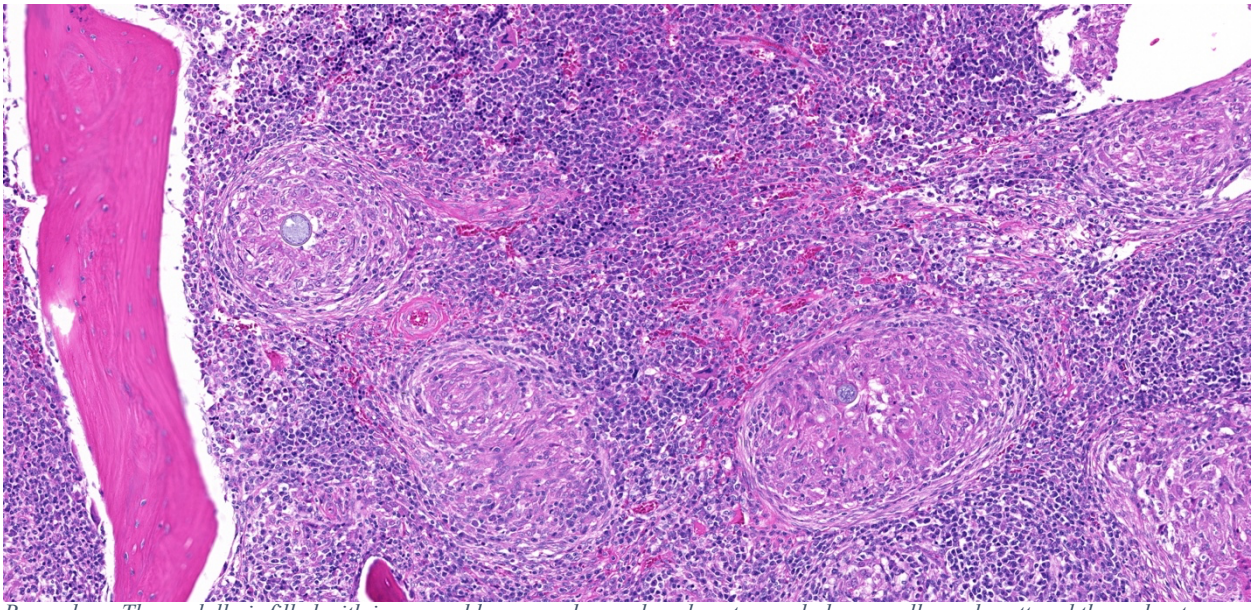

Bone, dog: The medulla is filled with innumerable macrophages, lymphocytes, and plasma cells, and scattered throughout are granulomas centered on 40-60um spherules with a thin hyaline wall and basophilic cytoplasm. (HE, 127X)

modalities including clinical suspicion based on physical exam, signalment, and history, routine bloodwork, radiographs, serology, and cytology or histopathology. Serological tests (including agar gel immunodiffusion, ELISA, and latex particle agglutination) can be specific, however they are typically insensitive and can produce false negative results.[6,8] Detection of antigen in urine or serum is also an insensitive test for diagnosis in dogs.[10] Therefore, cytological examination of trans-tracheal wash, bronchoalveolar lavage fluid, and fine needle aspirates and/or histopathological examination of affected tissues are often pursued to help provide a definitive diagnosis. Fungal culture is another diagnostic option; however, this procedure presents a hazard to laboratory personnel and should only be performed in properly equipped laboratories.[6,8]

Contributing Institution:
University of Illinois College of Veterinary Medicine, Veterinary Diagnostic Laboratory
http://vetmed.illinois.edu/vet-resources/veterinary-diagnostic-laboratory/

JPC diagnosis:
Bone: Osteomyelitis, granulomatous, diffuse, severe, with marked bone lysis and numerous endosporulating spherules, Yorkshire terrier, canine.

JPC comment:
The first documented case of coccidioidomycosis was in 1892 in an Argentinian soldier who presented with skin lesions. While it resembled mycosis fungoides, this soldier's lesions differed, and had rounded organisms at the center of lesions. Originally thought to be a protozoan, the name *Coccidioides* was given because of the similarities with coccidia. It wasn't until 8 years later that it was reclassified as a fungus, but the name remained the same.[2]

Coccidioides immitis and *Coccidioides posadasii* are indistinguishable via serology, they are morphologically identical, and their predicted proteins are >90% homologous. The largest factor for differentiating these two species is geography, with *C. immitis* found primarily in the desert regions of central and southern California, while *C. posadasii* is primarily found in desert regions of Nevada, Arizona, New Mexico, western Texas, Mexico, and Central and South America. There are significant genetic variations between the two species, allowing for differentiation.[9]

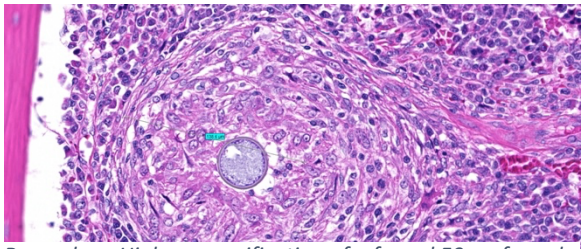

Bone, dog: Higher magnification of a fungal 50um fungal spherule within the center of a granuloma. (HE, 400X)

While there are gaps in knowledge regarding virulence factors, it has been shown that deletion of the gene coding for the spherule outer wall glycoprotein decreases virulence significantly. Ammonia metabolism is important for virulence as well, and *Coccidioides* spp synthesize a urease and ureidoglycolate hydrolase, allowing for the alkalization of the local environment. Additionally, the gene encoding carbamoyl phosphate synthetase, *CPS1*, appears to be significant to virulence, as deletion of the gene resulted in slow spherule growth, lack of endosporulation, and was avirulent in immunocompromised mice.[9]

The host response is multifactorial, but both innate and adaptive immune systems serve necessary functions of a successful response. Of the pattern recognition receptors (PRR), the most active in responding to the *Coccidioides* spp spherule wall are Toll-like receptors (TLR) and C-type lectin-like receptors (CLR). Specifically, the gene *Clec7a* encodes C-type receptor Dectin-1, a β-glucan receptor that responds to fungal cell walls. Downstream from Dectin-1 is caspase recruitment domain-containing protein 9 (Card9), which is an immune adaptor protein that activates Th1 and Th17 immunity against *Coccidioides* spp infection.[7]

The environment plays an important role in the ability of *Coccidioides* sp. to survive and proliferate. In areas with endemic Coccidioidomycosis, the soil has high levels of essential nutrients such as iron, calcium, and magnesium, regardless of soil pH. Animals carcasses may play an important role in the survival of this fungus as a medium for fungal growth, with isolates of *Coccidioides* sp. found around animal burrows, with no isolates found in areas with no animal activity.[4]

References:

1. Butkiewicz CD, Shubitz LF, Dial SM. Risk factors associated with Coccidioides infection in dogs. J Am Vet Med Assoc. 2005;226(11):1851-1854.
2. Chiller TM, Galgiani JN, Stevens DA. Coccidioidomycosis. *Infect Dis Clin N Am*. 2003;17:41-57.
3. Cox RA, Magee DM. Coccidioidomycosis: host response and vaccine development. Clin Microbiol Rev. 2004;17(4):804-839.
4. del Rocio Reyes-Montes M, Ameyali Perez-Huitron M, Luis Ocana-Monroy J, et al. The habitat of *Coccidioides* spp. and the role of animals as reservoirs and disseminators in nature. *BMC Infectious Diseases*. 2016;16:550.
5. Fisher MC, Koenig GL, White TJ, et al. Molecular and phenotypic description of Coccidioides posadasii sp. nov., previously recognized as the non-California population of Coccidioides immitis. Mycologia. 2002;94(1):73-84.
6. Graupmann-Kuzma A, Valentine BA, Shubitz LF, et al. Coccidioidomycosis in dogs and cats: a review. J Am Vet Med Assoc. 2008;44(5):226-235.
7. Hung CY, Hsu AP, Holland SM, Fierer J. A review of innate and adaptive immunity to coccidioidomycosis. *Medical Mycology*. 2019;57:S85-S92.
8. Johnson LR, Herrgesell EJ, Davidson AP, et al. Clinical, clinicopathologic, and radiographic findings in dogs with coccidioidomycosis: 24 cases (1995–2000). J Am Vet Med Assoc. 2003;222(4):461-466.
9. Kirkland TN, Fierer J. *Coccidiodes immitis* and *posadasii*; A review of their biology, genomics, pathogenesis, and host immunity. *Virulence*. 2018;9(1):1426-1435.
10. Kirsch EJ, Greene RT, Prahl A, et al. Evaluation of Coccidioides antigen detection in dogs with coccidioidomycosis. Clin Vaccine Immunol. 2012;19(3):343-345.
11. Nguyen C, Barker BM, Hoover S, et al. Recent advances in our understanding of the environmental, epidemiological, immunological, and clinical dimensions of coccidioidomycosis. Clin Microbiol Rev. 2013;26(3):505-525.
12. Shubitz LF, Butkiewicz CD, Dial SM, et al. Incidence of Coccidioides infection among dogs residing in a region in which the organism is endemic. J Am Vet Med Assoc. 2005;226(11):1846-1850.
13. Shubitz LF. Comparative aspects of coccidioidomycosis in animals and humans. Ann N Y Acad Sci. 2007:1111:395-403.

CASE 3: MSU Case#1 (4065133-00)

Signalment: 3.5-year-old, male, white-tailed deer, *Odocoileus virginianus*

History:
This buck was harvested by a hunter during rifle season. He submitted the deer for examination because of skin lesions.

Gross Pathology:
The skin over the muzzle, face, ears, and limbs had patchy areas of thickening, alopecia, and crusts. On cross-sections of affected skin, numerous round to elongate, pale, 2-5mm diameter nodules were visible. In addition, the subcutaneous tissues of the muzzle were diffusely swollen and edematous.

Laboratory results:
PCR testing for BVD on spleen was negative. PCR on pooled lung, liver and spleen for Epizootic Hemorrhagic Disease virus was negative. Immunohistochemical staining of obex and retropharyngeal lymph nodes for Chronic Wasting Disease prion protein was negative.

Microscopic description:
Sections of skin contained markedly ectatic hair follicles filled with myriads of cigar-shaped arthropod parasite adults, nymphs, larva and eggs. Adults measured 140-180µm long, 25-40µm diameter, with 4 pairs of stubby legs, and contained striated muscles internally. Follicles exhibited loss of hair shafts, moderate hyperkeratosis, secondary bacterial colonization, with predominantly lymphoplasmacytic folliculitis. Some hair follicles had ruptured resulting in granulomatous to pyogranulomatous furunculosis associated with mites outside of the hair follicles. Overlying epidermis was moderately thickened, with rete peg formation, orthokeratotic hyperkeratosis, and variable amounts of serocellular crusting. The dermis was expanded by mixed lymphoplasmacytic, eosinophilic, and neutrophilic infiltrates.

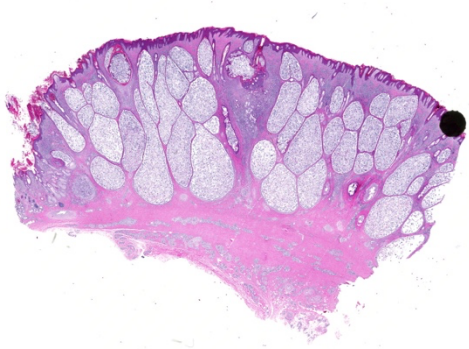

Haired skin, white-tailed deer: Hair follicles are markedly dilated, and the epithelium is mildly hyperplastic and hyperkeratotic. (HE, 5X)

Contributor's morphologic diagnosis:
Skin: severe follicular ectasia, with lymphoplasmacytic folliculitis and granulomatous furunculosis, and numerous intra-follicular arthropod mites consistent with *Demodex* sp.

Contributor's comment:
Demodicosis is a fairly straightforward histologic diagnosis in most severely affected individuals in many different species of animal. The species of demodectic mite most commonly reported in white-tailed deer is *Demodex odocoilei*. Other species of deer known to be affected by this parasite include mule deer and black-tailed deer.[3,5] European deer species including red deer, roe deer, Sambar deer and sika deer are reported to be infested with *Demodex kutzeri*.[3] While the mites in this report are in the right size range reported for nymphs of *Demodex odocoilei*, no specific molecular identification was performed.[3]

The degree of mite infestation in this case is impressive. While I have examined a number of deer cases with demodicosis, I have never encountered one with grossly visible ectatic follicles, although other authors have reported these nodules.[5] I would estimate that there were several hundred organisms per infected hair follicle. One recent paper cites an estimate of 6.3 mites per hair follicle. Another unusual feature was the grossly swollen edematous muzzle in this animal. My colleagues in the MI Department of Natural Resources have seen this several times and refer to this as the "Bullwinkle J. Moose Syndrome", since the muzzle appears bulbous and swollen as naturally occurs in moose. I know

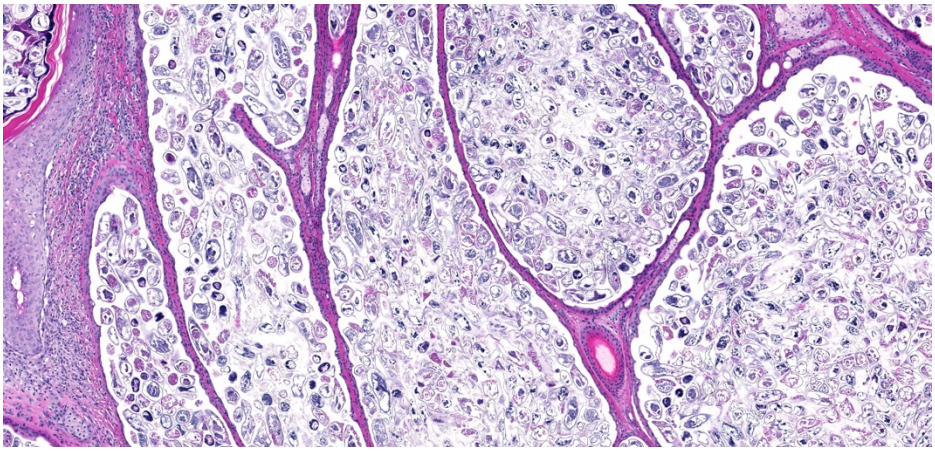

Haired skin, white-tailed deer: Dated hair follicles contain numerous cross sections of arthropod parasites. (HE, 66X)

of no reported explanation for this syndrome, nor of its occurrence in any other mammalian species in association with demodicosis infestations. Possible pathogeneses may include secondary bacterial infection of the follicles and skin leading to a local bacterial toxin release, or follicular ectasia and granulomatous furunculosis leading to physical obstruction of lymphatic drainage causing secondary subcutaneous edema.

The severe degree of pathology associated with this case is atypical for demodicosis. Therefore, we considered underlying immunosuppression as occurs in some cases of generalized canine demodicosis. However, fecal examination failed to reveal heavy gastrointestinal parasitism, examination of lymph nodes and lungs revealed no gross or microscopic evidence of bovine tuberculosis (endemic in MI deer), and testing for BVD, CWD and EHD were all negative. Furthermore, the deer was not in poor body condition. However, similar to previous reports, this deer was a male, was harvested in the fall and that time period coincides with breeding season and increases in hormones such as testosterone and cortisol, which may have increased this individual's susceptibility to developing clinical demodicosis.[5]

Contributing Institution:
Department of Pathobiology
College of Veterinary Medicine
Michigan State University
www.pathobiology.msu.ed

JPC diagnosis:
Haired skin: Follicular ectasia, diffuse, severe, with multifocal lymphohistiocytic dermatitis, folliculitis, and furunculosis, and myriad intrafollicular mite adults, nymphs, and eggs, white-tailed deer, cervid.

JPC comment:
During conference discussion, there was debate in how best to represent the processes taking place in this tissue. While the furunculosis was a granulomatous process, the dermatitis and folliculitis were of a predominately lymphocytic nature. It was also noted that some slides had focal sarcocysts in the subjacent musculature.

The first reported case of *Demodex* sp. in the white-tailed deer was in the 1960's, in Georgia, though speciation was not performed. However, a novel *Demodex* species of white-tailed deer was first described in detail in 1974, including detailed measurements, images of all life stages, and descriptions of several pathogenic manifestations of disease. This novel species was named *Demodex odocoilei*, and as previously described by the contributor, has been a common finding in white-tailed deer. This is one of a small subset of *Demodex* species that has been found invading local blood vessels.[1,2]

While usually host-specific, species of *Demodex* have been found on different species, including

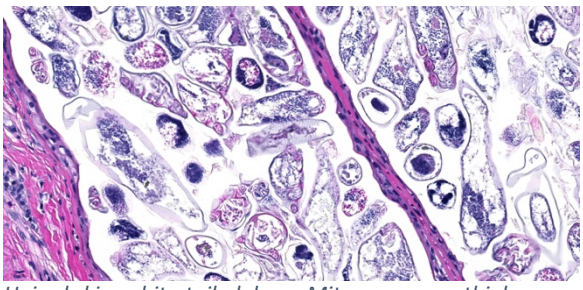

Haired skin, white-tailed deer: Mites possess a think chitinous exoskeleton, jointed appendages (arrows), and skeletal muscle. (HE, 400X)

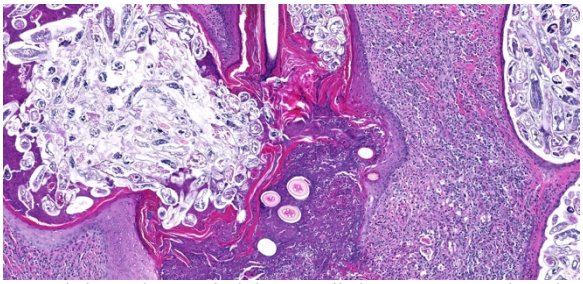

Haired skin, white-tailed deer: Follicles are ruptured, with a profound granulomatous response to liberated mites, hair shafts, and keratin debris. (HE, 93X)

Demodex kutzeri on white-tailed deer, and *Demodex odocoilei* in Columbian black-tailed deer (*Odocoileus hemionus columbianus*) and mule deer (*Odocoileus hemionus* hemionus). A third species of *Demodex* affecting white-tailed deer was detailed in 2013, with physical parameters and phylogenetic analysis distinguishing it from *D. odocoilei*. In cases with this new *Demodex* species, there were multiple 1-2 cm tan cutaneous nodules on the head, legs, and lateral thorax and abdomen, but without alopecia. Histologically, nodules were determined to contain several hundreds to thousands of intrafollicular *Demodex* mites. There was mild perifollicular lymphocytic and histiocytic dermatitis, but significant inflammation was only present in cases of furunculosis.[7]

Because *Demodex* spp are generally thought to be species-host specific, it is curious that we find *Demodex* species that exist on different host species. Phylogenetic analysis estimates that *Demodex kutzeri* from elk and *D. folliculorum* from humans had a common ancestor approximately 85 million years ago. This coincides with the divergence of the two host species, with their common ancestor diverging approximately 84 million years ago. However, when morphologically similar *D. kutzeri* from elk and mule deer were compared, they had extremely low levels of sequence divergence, suggesting a single species. However, elk and mule deer diverged from each other approximately 7 million years ago. Very few genetic sequences of *Demodex* have been completed, but in the future may help determine 1) previously unknown species of *Demodex*, or 2) mechanisms by which they perform host-switching.[6]

References:

1. Carpenter JW, Freeny JC, Patton CS. Occurrence of *Demodex* Owen 1843 on a white-tailed deer from Oklahoma. *Journal of Wildlife Diseases*. 1972;8:112-114.
2. Desch CE, Nutting WB. *Demodex odocoilei* sp. nov. from the white-tailed deer, *Odocoileus virginianus*. *Can. J. Zool*. 1974;52:785-789.
3. Gentes ML, Proctor H, Wobeser G. Demodicosis in a mule deer (Odocoileus hemiones hemiones) from Saskatchewan, Canada. *J Wildl Dis* 2007;**43:**758-761.
4. Howerth EW, Nemeth NM, Ryser-Degiorgis MP. Cervidae. In: eds. Terio KA, McAloose D, St. Leger J. *Pathology of Wildlife and Zoo Animals*. Elsevier: San Diego, CA. 2018:174.
5. Nemeth NM, Ruder MG, Gerhold RW, et al. Demodectic mange, dermatophilosis, and other parasitic and bacteriologic diseases in free-ranging white-tailed deer (*Odocoileus virginianus*) in the United States from 1975 to 2012. *Vet Pathol* 2013;**51:**633-640.
6. Palopoli MF, Tra V, Matoin K, Mac PD. Evolution of host range in the follicle mite *Demodex kutzeri*. *Parasitology*. 2017;144(5):594-600.
7. Yabsley MJ, Clay SE, Gibbs SEJ, Cunningham MW, Austel MG. Morphologic and molecular characterization of a *Demodex* (Acari: Demodicidae) species from white-tailed deer (*Odocoileus virginianus*). *ISRN Parasitology*. 2013;342918.

CASE 4: L16758 (4114759-00)

Signalment: 16-year-old, female, serval (*Leptailurus serval*)

History:

The animal was presented to the Baton Rouge zoo's veterinary hospital for recurrent hematuria, pollakiuria and intermittent anorexia. Interpretation of abdominal ultrasound revealed thickening of the urinary bladder wall (image capture was not available). Hematuria and pyuria were confirmed via free catch urinalysis, with

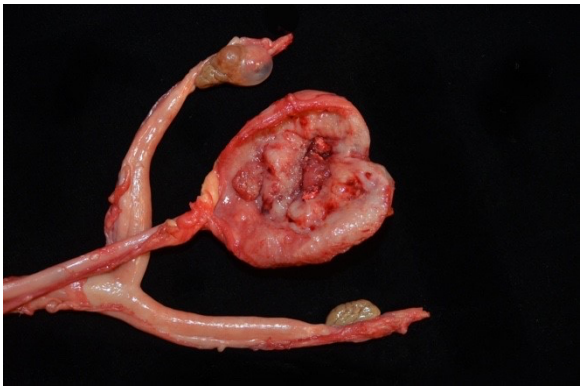

Urinary bladder, serval: The wall of the urinary transmurally expanded by a pale tan-to-red, multinodular, exophytic, infiltrative, poorly demarcated neoplasm measuring 3.5 x 3.0 x 0.6cm. (Photo courtesy of: Boston University/NEIDL 620 Albany Street, Boston, MA, 02118).

hematuria refractory to antimicrobial therapy. Due to persistent anorexia resulting in significant weight loss and an overall loss in the quality of life the serval was humanely euthanized.

Gross Pathology:

Approximately 80% of the urinary bladder body was transmurally expanded by a pale tan-to-red, multinodular, infiltrative, poorly demarcated neoplasm measuring 3.5 x 3.0 x 0.6cm**.** Abdominal adipose tissue was segmentally adhered to the ventral adventitial surface of the urinary bladder. The lumen of the urinary bladder was devoid of urine and no significant free fluid was observed in the peritoneal cavity. No evidence to support urinary obstruction (i.e. hydroureter and hydronephrosis) were observed. A yellow fluctuant paraovarian cyst measuring 1.2 cm in diameter was present along the cranial pole of the right ovary. Kidneys were interpreted as within normal limits grossly.

Laboratory results:

A cytospin preparation of urine sediment (free catch) revealed 1-3 epithelial cells per high power field, some of which displayed moderate atypia including increased cytoplasmic basophilia, variable and increased nucleus:cytoplasm ratio, anisokaryosis, rare multinucleation, and prominent nucleoli. Serum biochemistry findings included hyperproteinemia with hyperglobulinemia, marginal azotemia, hyperphosphatemia, hyponatremia, hypochloremia, decreased NA:K ratio, hyperkalemia, and hyperamylasemia. Significant urinalysis findings included inappropriately concentrated urine in the face of a clinically dehydrated animal, proteinuria, hematuria, and pyuria.

Serum Biochemistry		
Analyte	Result	Reference Interval
Total protein	8.9	5.0-7.8 g/dL
Globulins	5.2	1.7-4.7 g/dL
Creatinine	14.2	0.8-3.4 mg/dL
BUN	51	20-50 mg/dL
Phosphorus	18.9	3.6-10.4 mg/dL
Sodium	134	144-163 mEq/L
Chloride	90	109-129 mEq/L
NA:K ratio	23	26.4-44
Potassium	5.9	3.5-5.5 mEq/L
Amylase	1,424	243-1,049 U/L
Urinalysis (free catch)		
Specific gravity	1.014	Dehydrated
Protein	1+	
Blood	3+	
RBC	25-50 RBC/low power field	
WBC	1-3 WBC/low power field	

Microscopic description:

Urinary bladder neoplasm: Arising from transitional urothelium, infiltrating the propria-submucosa and muscularis, with extension into the adventitia and adjacent peritoneal adipose tissue is a raised, non-papillary, infiltrative, unencapsulated, moderately-to-densely cellular neoplasm**.** Neoplastic cells are composed of cuboidal-to-columnar epithelial cells arranged in acini, tubules, and trabeculae, which are supported by a moderate-to-dense fibrovascular stroma (desmoplasic/scirrhous response). Neoplastic cells have variably distinct cellular

Urine cytospin, serval: Epithelial cells display moderate atypia including cytoplasmic basophilia, variable and increased N/C ratio, anisokaryosis, rare multinucleation, and prominent nucleoli. (Photo courtesy of: Boston University/NEIDL 620 Albany Street, Boston, MA, 02118).

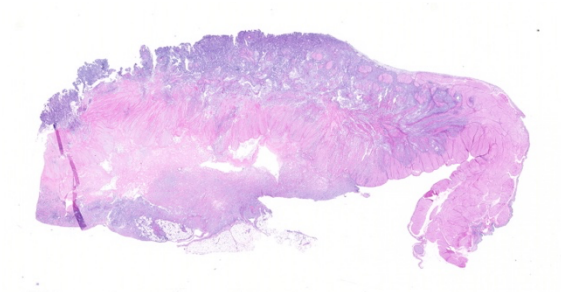

Urinary bladder, serval: The neoplastic mucosa is exophytic and papillary, and a moderately cellular neoplasms transmurally infiltrates the bladder wall. (HE, 5X)

borders, a moderate amount of granular eosinophilic cytoplasm, round to oval nuclei with finely stippled chromatin, and 1-2 prominent centrally located magenta nucleoli. Anisocytosis and anisokaryosis are moderate, with 20 mitotic figures per 10 high powered fields. Neoplastic cells display strong cytoplasmic chromogenic immunoreactivity to cytokeratin AE1/AE3, with loss of cytokeratin 7 immunoreactivity when compared to neighboring surface transitional epithelium. Uroplakin III and cytokeratin 20 antibodies were not available for evaluation. Large areas of mural necrosis are represented by lakes of amorphous hypereosinophilic cellular debris and are commonly admixed with foci of basophilic mineralization (dystrophic). Vascular invasion was not observed in the sections examined; however, multiple microscopic foci of pulmonary metastasis were observed expanding alveolar septa.

Kidney (not depicted in submitted slide): The interstitium is expanded multifocally by mild fibrosis associated mild tubular degeneration and atrophy. Some tubules contain large clear spaces within the lumina (lipid casts). Lymphoplasmacytic and histiocytic inflammation surrounds these foci. Some tubules have ruptured resulting in the release of intraluminal lipid content into adjacent interstitium, associated with accumulation of lipid laden macrophages (lipogranulomatous inflammation).

Contributor's morphologic diagnosis:
Urinary bladder: Urothelial carcinoma, non-papillary, infiltrative, with pulmonary micrometastasis (not evident in submitted slide)

Kidneys: Nephritis, tubulointerstitial, lipogranulomatous, with interstitial fibrosis, lipid casts, tubular degeneration and atrophy, mild, chronic

Contributor's comment:
Urothelial carcinomas of the urinary bladder are classified as papillary or non-papillary and as infiltrating or non-infiltrating. Papillary tumors project into the lumen of the urinary bladder,

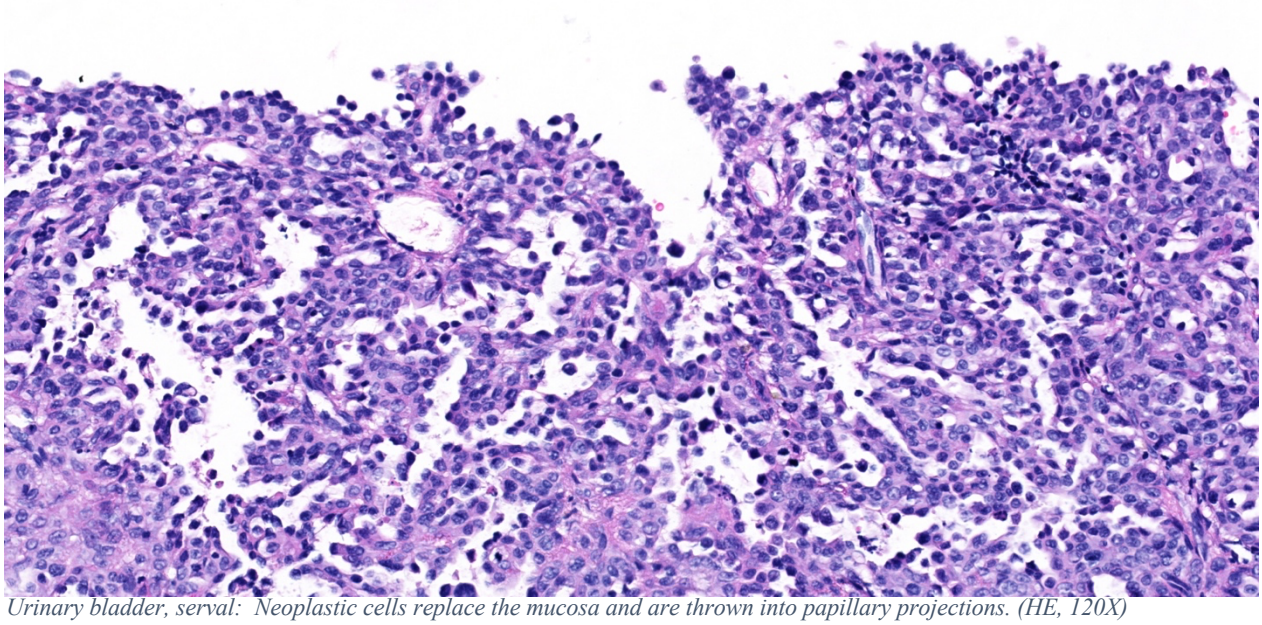

Urinary bladder, serval: Neoplastic cells replace the mucosa and are thrown into papillary projections. (HE, 120X)

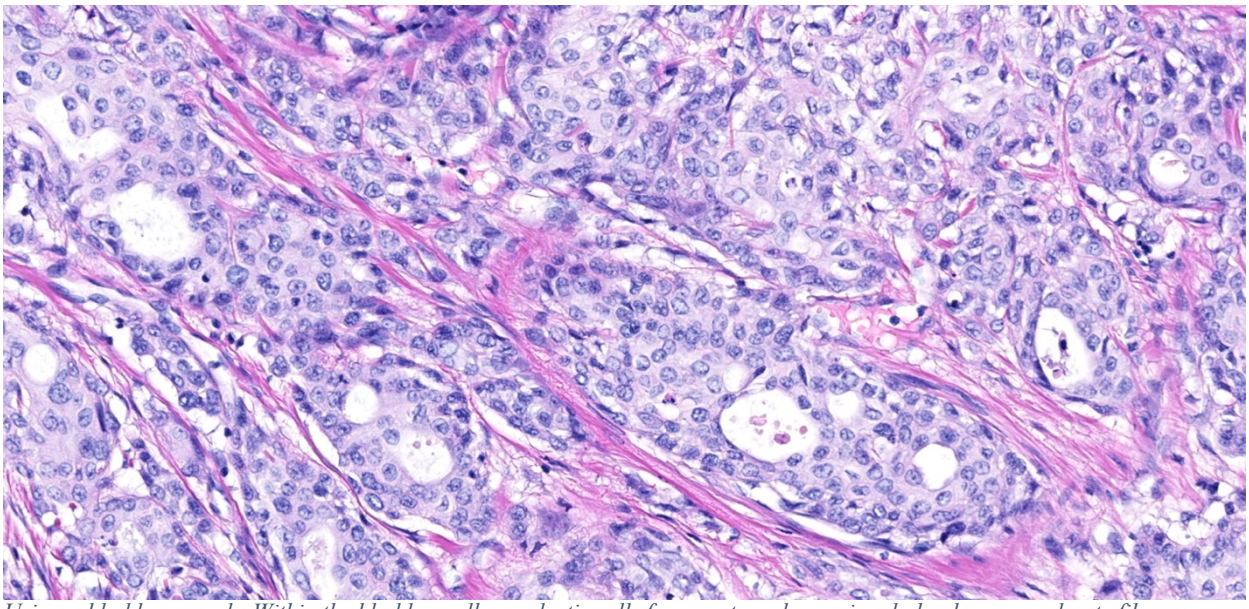

Urinary bladder, serval: Within the bladder wall, neoplastic cells form nests and occasional glands on a moderate fibrous stroma (HE, 340X)

while non-papillary tumors often are either flat or fail to form a discrete exophytic mass. Infiltrating tumors are characterized by extension into the underlying substantia propria and muscularis, with occasional transmural involvement; meanwhile non-infiltrating tumors do not invade the substantia propria. Non-papillary infiltrative tumors are most likely to metastasize, followed by papillary infiltrative tumors. Metastasis is not likely with papillary non-infiltrative tumors. Non-papillary non-infiltrative tumors are synonymous with carcinomas in situ and are confined to the surface epithelium. Histologic features that may suggest an increased likelihood of metastasis include marked cellular atypia, prominent muscular invasion and/or desmoplastic response, and the presence of vascular invasion.[4] Metastasis is most commonly reported to regional lymph nodes, lungs, and bones, but peritoneal and cutaneous implantation have been documented.

Urothelial carcinoma represents the most common urinary bladder neoplasm of both cats and dogs with similar reported frequencies. In dogs, females are overrepresented with up to a 2:1 ratio reported in multiple studies.[7] Additionally, neutered dogs, independent of sex, are more commonly affected than intact dogs.[6] In cats, this predilection for neutered animals has not been consistently observed and one study identified male cats to be at an increased risk when compared to female cats. Several breed dispositions have been identified, including Scottish Terriers, Airedales, Shetland Sheepdogs, Beagles, Collies, Wire Hair Fox Terriers, and West Highland White Terriers[4,6], meanwhile no breed predilection has been identified in domestic cats. Risk factors for development of urinary bladder urothelial carcinoma are best described in dogs, which include exposure to topical insecticides, obesity, and administration of cyclophosphamide; meanwhile second hand smoke has not been proven to represent a risk factor as is reported in humans.[2,6] In cattle, spontaneous tumor development of the urinary bladder is uncommon; however, up to 25% of animals known to graze pasture rich in bracken fern have been reported to develop urinary bladder tumors including urothelial carcinoma.[8] Bracken fern contains ptaquiloside, a known carcinogen, which is believed to act synergistically with Bovine papillomavirus type-2 (BPV-2) to cause neoplastic transformation.

Initially this animal was presumed to be suffering from chronic recurrent bacterial cystitis, as hematuria was initially responsive to antimicrobial treatment. Hematuria ultimately became refractory to treatment and ancillary

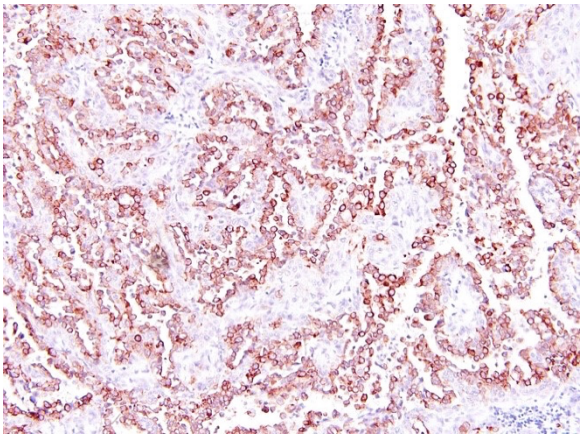

Urinary bladder: Neoplastic cells demonstrate strong cytokeratin cytoplasmic immunoreactivity (anti AE1/AE3, 40X)

diagnostics were pursued (i.e. ultrasound and urine sediment interpretation). Interpretation of these diagnostics placed urothelial carcinoma as the top differential. Serum biochemistry findings were in part attributed to the clinically appreciated dehydration, manifesting as pre-renal disease (i.e. azotemia, hyperphosphatemia). The immediate cause of the hyperkalemia, hyponatremia and hypochloremia were unknown, as the animal clinically had no history of vomiting or diarrhea in the face of dehydration. Although the collective electrolyte abnormalities (i.e. hyperkalemia, hyponatremia, and hypochloremia) were highly suggestive of urine and blood equilibration through the peritoneum (i.e. uroperitoneum), no appreciable free abdominal fluid was identified at the time of necropsy. If free fluid was present in the peritoneum at the time of necropsy, ascitic fluid levels of creatinine would have been expected to be markedly higher than those in the blood. In the absence of discrete abdominal fluid and an alternative explanation, we propose that adventitial plugging of the urinary bladder by adipose tissue resulted in a slow, controlled, and chronic release of urine into the abdomen that was able to equilibrate at a rate where accumulation of fluid was no appreciable at necropsy. Inadequate urine concentrating capacity in the face of dehydration (urine specific gravity of 1.014; expect ≥ 1.035 in a dehydrated feline) supports concomitant renal disease, which is believed to have played a contributory role in the electrolyte disturbances and azotemia observed in this case. Lipogranulomatous inflammation has been documented in domestic cats after various types of renal insults such as experimental ischemia reperfusion injury and nephrotoxicity. Tubular injury and tubulorhexis can lead to release of intraepithelial lipid into the interstitium, which incites a granulomatous inflammatory response. This inflammation can then perpetuate further renal injury by expansion of the interstitium and compression of the peritubular capillaries.[9] Planet Earth, Season 2, Grasslands showcases the serval in its natural habitat.

Contributing Institution:
Boston University/NEIDL 620 Albany Street, Boston, MA, 02118

JPC diagnosis:
Urinary bladder: Urothelial (transitional) cell carcinoma, serval, feline.

JPC comment:
During conference discussion, it was noted that different sections had different predominant patterns, including features of non-papillary, infiltrative, or papillary, infiltrative.

While not all urothelial carcinomas share a common cause, approximately 80% of canine urothelial carcinomas are associated with mutation in the *BRAF* V595E allele. This allele in dogs is homologous to BRAF V600E mutation in humans, which is found in approximately 50% of human melanomas.[10] Point of care tests are currently performed on voided urine, and one successful method is the digital droplet PCR test (ddPCR). Even though approximately 20% of canine cases of urothelial carcinoma do not possess the mutation, the ddPCR test has a sensitivity around 80%.[5]

While the BRAF mutation testing is not available for cats yet, additional work has been performed to characterize the expression of cyclo-oxygenase 1 (COX-1), cyclo-oxygenase 2 (COX-2), lipoxygenase 5 (LOX-5), and human epidermal growth factor receptor 2 (HER2). A small study of feline urothelial carcinomas showed that most expressed COX-1 and COX-2, and that the

neoplasms responded to the COX inhibitor meloxicam, with increased mean survival times.

LOX-5 over-expression has been linked to human neoplasia, including prostatic, renal, and bladder cancer. LOX-5 has a pro-inflammatory effect, activated by nF-KB, and leading to sustained angiogenesis through induction of VEGF, cell migration, invasion, and resistance to apoptosis by inhibition of caspase 3. An investigation into canine urothelial carcinomas showed that 95% of tumors expressed LOX-5. Additionally, canine urothelial carcinomas also express COX-2, which is generally not expressed in normal canine bladder urothelium.[1]

Increased receptor tyrosine kinase HER2 activity has been shown in a subset of human breast cancers, as is a recent target of interest for canine urothelial carcinomas. While increased HER2 expression correlates with a poorer prognosis, no correlations between HER2 expression and age, sex, sexual status, tumor size, tumor T stage, lymph node involvement, distant metastasis, or recurrence in canine urothelial carcinomas. However, there was increasing HER2 expression across groups, from polypoid cystitis, to grade 1 carcinoma, to grade 2 carcinoma. Grade 3 urothelial carcinomas had decreased HER2 expression than in grades 1 and 2, which may represent dedifferentiation of neoplastic cells and may be analogous to the loss of uroplakin III expression in grade 3 urothelial carcinomas.[11]
The UPII-SV40T strain of transgenic mice are a model for urothelial carcinoma, as they develop invasive urothelial tumors due to expression of Simian virus large T antigen (Tag). Most often, these tumors are classified as high grade, invasive carcinomas by 40 weeks of age. The chemopreventive, licofelone, is a dual COX-2 and LOX-5 inhibitor, which has been shown to prevent human colon, lung, and prostate cancers. Mice fed licofelone developed fewer invasive, and fewer high-grade urothelial carcinomas, and may represent a future treatment for other species.[3]

References:

1. Finotello R, Schiava L, Ressel L, Frohmader A, Silvestrini P, Verin R. Lippoxygenase-5 expression in canine urinary bladder: Normal urotherlium, cystitis and transitional cell carcinoma. *J Comp Path*. 2019;170:1-9.
2. Landolfi JA, Terio KA. Transitional cell carcinoma in fishing cats (*Prionailurus viverrinus*): Pathology and expression of cyclooxygenase-1, -2, and p53. *Vet Pathol* 2006;43:674-681.
3. Madka V, Mohammed A, Li Q, et al. Chemoprevention of urothelial cell carcinoma growth and invasion by the dual COX-LOX inhibitor licofelone in UPII-SV40T transgenic mice. *Cancer Prev Res (Phila)*. 2014;7(7):708-716.
4. Meuten DJ. Tumors of the Urinary System. In: Meuten DJ. *Tumors of Domestic Animals*. 4th ed. Ames: Iowa State Press. 2002; 529-535.
5. Mochizuki H, Shapiro SG, Breen M. Detection of BRAF mutation in urine DNA as a molecular diagnostic for canine urothelial and prostatic carcinoma. *PLoS ONE*. 2015;10(12):e0144170.
6. Mutsaers AJ, Widmer WR, Knapp DW. Canine transitional cell carcinoma. *J Vet Intern Med* 2003;17:136–144.
7. Norris AM, Laing EJ, Valli VEO, et al. Canine bladder and urethral tumors: a retrospective study of 115 cases (1980-1985). *J Vet Intern Med* 1992;6:145-153.
8. Pamukcu AM, Price JM, Bryan GT. Naturally occurring and braken-fern-induced bovine urinary bladder tumors. Clinical and morphological characteristics. *Vet Pathol* 1976;13(2):110-22
9. Schmiedt CW, Brainard BM, Hinson W, et al. Unilateral renal ischemia as a model of acute kidney injury and renal fibrosis in cats. *Vet Pathol* 2016;53:87-101.
10. Tagawa M, Tambo N, Maezawa M, et al. Quantitative analysis of the BRAF V595E mutation in plasma cell-free DNA from dogs with urothelial carcinoma. *PLoS ONE*. 2020;15(4):e0232365.
11. Tsuboi M, Sakai K, Maeda S. Assessment of human epidermal growth factor receptor 2 expression in canine urothelial carcinoma of the urinary bladder. *Veterinary Pathology*. 2019;56(3):369-376.